BCSJ

Document type: Article

Cembranoid-Related Diterpenes, Novel Secoditerpenes, and an Unusual Bisditerpene from a Formosan Soft Coral *Sarcophyton Tortuosum*

Kuan-Hua Lin,[1,#] Yu-Chi Lin,[1,#] Chiung-Yao Huang,[1] Yen-Ju Tseng,[1] Shu-Rong Chen,[2] Yuan-Bin Cheng,[1,2] Tsong-Long Hwang,[3,4,5] Sheng-Yang Wang,[6] Hsing-Yin Chen,[7] Chang-Feng Dai,[8] and Jyh-Horng Sheu*[1,2,9]

[1]Department of Marine Biotechnology and Resources, National Sun Yat-sen University, Kaohsiung 80424, Taiwan

[2]Graduate Institute of Natural Products, College of Pharmacy, Kaohsiung Medical University, Kaohsiung 80708, Taiwan

[3]Graduate Institute of Natural Products, Graduate Institute of Biomedical Sciences, College of Medicine, Chang Gung University, Taoyuan 33302, Taiwan

[4]Research Center for Industry of Human Ecology, Research Center for Chinese Herbal Medicine, and Graduate Institute of Health Industry Technology, College of Human Ecology, Chang Gung University of Science and Technology, Taoyuan 33302, Taiwan

[5]Department of Anesthesiology, Chang Gung Memorial Hospital, Taoyuan 33302, Taiwan

[6]Department of Forestry, National Chung Hsing University, Taichung 402204, Taiwan

[7]Department of Medicinal and Applied Chemistry, Kaohsiung Medical University, Kaohsiung 807, Taiwan

[8]Institute of Oceanography, National Taiwan University, Taipei 112216, Taiwan

[9]Department of Medical Research, China Medical University Hospital, China Medical University, Taichung 404332, Taiwan

E-mail: sheu@mail.nsysu.edu.tw

Received: July 21, 2021; Accepted: September 17, 2021; Web Released: October 5, 2021

Jyh-Horng Sheu

Jyh-Horng Sheu received his Ph.D. degree from University of California, San Diego in 1985. He has been working at the Department of Marine Biotechnology and Resources, National Sun Yat-sen University since the completion of his Ph.D. study, and appointed to Director of Frontier Center for Ocean Science and Technology from 2012–2020 and to Distinguished Professor in 2016. His research interests are focused on the chemistry of marine natural products, organic synthesis, and drug discovery.

Abstract

Further chemical investigation of the ethyl acetate extract of the soft coral *Sarcophyton tortuosum* has led to the isolation of ten terpenoidal metabolites, including six new compounds, secoditerpenes secotortuosenes A and B (**1** and **2**), diterpenes tortuosenes C and D (**3** and **4**) and tortuosumol (**5**), and a biscembranoid bisotortuolide cyclobutane A (**6**), along with four known compounds, ketoemblide (**7**), sartrolide G (**8**), emblide (**9**), and sarcrassin E (**10**). Compounds **5** and **6** are metabolites of intra- and intermolecular [2+2] cyclizations, respectively. Notably, **1** and **2** are 12-membered carbocyclic compounds possessing a 2-methyl-3-oxopentanyl side chain and representing an unprecedented molecular skeleton, while compound **6** possesses a unique cyclobutanyl biscembranoid skeleton. The absolute configurations of **1** and **5** were determined by TDDFT ECD calculations. Bioassays showed that compound **5** exhibited selective cytotoxicity against the growth of the Molt-4 cell line, while **6** exhibited inhibitory activity against P388, K562, and HT-29 cancer cell lines. Compounds **3** and **5**–**7** showed effects for inhibition toward the generation of superoxide anion, while **3**, **6**, and **7** displayed inhibition activity against elastase release in fMLF/CB-induced neutrophils. In addition, compounds **6**, **7**, and **10** exhibited anti-inflammatory activity by inhibiting nitric oxide generation in the LPS-induced RAW 264.7 cell assay.

Keywords: *Sarcophyton tortuosum* | Anti-inflammatory | Cytotoxicity

1. Introduction

Soft corals (phylum, Cnidaria; class, Anthozoa; subclass,

Octocorallia; order, Alcyonaceae; family, Alcyoniidae) are important structural components of coral reef communities and contributors of coral reef biomass.[1,2] It is believed that these important marine organisms produce and release chemical substances to defend themselves against predators and reef competitors due to their soft-bodied and sessile nature.[3,4] The soft coral genus *Sarcophyton* is one of the most important organisms to produce secondary metabolites, found mainly in shallow waters of oceans all over the world.[5–10] Secondary metabolites such as diterpenes,[11–14] sesquiterpenes[15,16] and biscembranoids,[12,17,18] as well as several miscellaneous compounds including polyhydroxysterols[19] were found in corals of the *Sacrophyton* genus. Among the natural compounds discovered from soft corals, many cembranoids showed a broad spectrum of biological activities, including antitumor,[20,21] anti-inflammatory,[22,23] and neuroprotective activities.[24] Thus, it is important to discover more secondary metabolites from soft corals for future marine drug research and development.

In continuation of our chemical investigation for bioactive or structurally interesting metabolites of the soft coral *S. tortuosum* collected from Lanyu Island,[23] we continuously investigated the chemical constituents of this soft coral resulting in the isolation of two compounds with a novel secoditerpenodal skeleton secotortuosenes A and B (**1** and **2**), two new tortuosane diterpenoids tortuosenes C and D (**3** and **4**), one tricarbocyclic cembranoidal diterpenoid tortuosumol (**5**) with a rarely found tetradecahydrocyclopenta[3′,4′]cyclobuta-[1′,2′:4,5]cyclonona[1,2-*b*]-oxirene ring system, and a novel cyclobutane biscembranoid (**6**), as well as four known compounds, ketoemblide (**7**),[25] sartrolide G (**8**),[26] emblide (**9**),[25,27] and sarcrassin E (**10**) (Figure 1).[28] Structure elucidation of the new isolates was conducted by detailed spectroscopic analysis, including 2D NMR experiments (COSY, HSQC, HMBC, and NOESY) and comparison of spectroscopic data with related compounds. Biological activities including cytotoxicity and anti-inflammatory activity of these isolates are also reported herein.

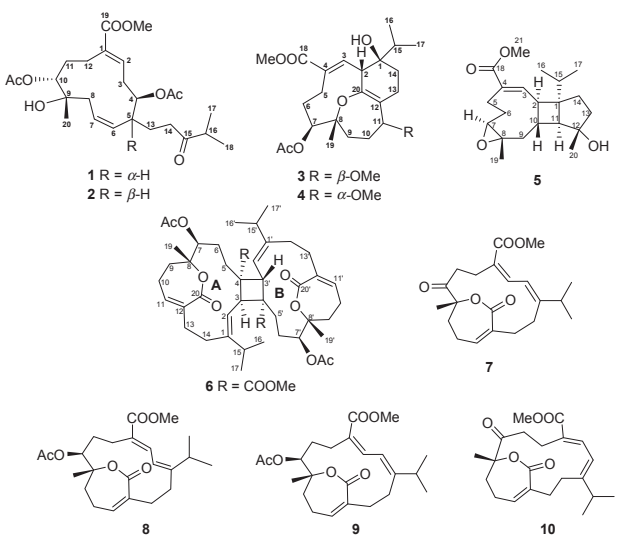

Figure 1. The chemical structures of **1**–**10** isolated from *S. tortuosum*.

2. Results and Discussion

Secotortuosene A (**1**) was obtained as a white amorphous powder with $[\alpha]_D^{25}$ +22.2 (*c* 0.8, $CHCl_3$). The molecular formula of $C_{25}H_{38}O_8$ was determined from the sodiated ion peak of HRESIMS at *m*/*z* 489.2462 $[M + Na]^+$ (calcd for $C_{25}H_{38}O_8Na$, 489.2464), indicating seven degrees of hydrogen deficiency. Its IR spectrum showed the presence of hydroxy (3496 cm^{-1}) and carbonyl (1738 cm^{-1}) groups. With the aid of HSQC spectrum, the ^1H NMR spectrum (Table 1) exhibited resonances corresponding to one isopropyl methyl group at δ_H 1.06 (d, $J = 6.8$ Hz, 6H), three methyl singlets (δ_H 1.27, 2.11, and 2.14) of which two are arisen from acetoxy groups, one methoxyl (δ_H 3.73), and three olefinic protons resonating at δ_H 6.74 (dd, $J = 10.4$ and 6.0 Hz), 5.58 (dt, $J = 11.2$ and 2.8 Hz), and 5.69 (dd, $J = 11.2$ and 10.0 Hz). The ^{13}C and DEPT spectra (Table 2) showed the presence of one di- and one trisubstituted double bonds [δ_C 126.8 (CH) and 129.8 (CH); 135.2 (C) and 137.2 (CH)], two acetoxy groups (δ_C 170.5, C and 21.1, CH_3; 170.7, C and 21.0, CH_3), one additional ester carbonyl (δ_C 167.6), and one keto carbonyl (δ_C 214.2), accounting for the presence of six double bonds and indicating that **1** is a monocyclic compound. The above evidence suggested that **1** might be a diterpenoid. The gross skeleton of **1** was established by the COSY and HMBC spectra (Figure 2). Analysis of the COSY spectrum led to the establishment of five separate proton spin systems, including H-2/H_2-3/H-4, H-5/H-6/H-7/H_2-8, H-10/H_2-11/H_2-12, H_2-13/H_2-14, and H_3-17/H-16/H_3-18, which were connected by HMBC correlations from H_2-12 (δ_H 2.21 and 2.43) to C-1 (δ_C 135.2, C) and C-2 (δ_C 137.2, CH), H_2-3 (δ_H 2.26 and 2.68) to C-5 (δ_C 39.8, CH), H_3-20 (δ_H 1.27) to C-8 (δ_C 39.2, CH_2) and two oxygen-bearing carbons C-9 (δ_C 74.4, C) and C-10 (δ_C 79.4, CH), to establish the 12-membered ring system of **1**. Additionally, HMBC correlations from H_2-13, H_2-14, H-16, H_3-17, and H_3-18 to ketocarbonyl carbon C-15 (δ_C 214.2), and from H-13 (δ_H 1.58) to C-5 allowed the linkage of 2-methyl-3-oxopentanyl group to the 12-membered ring at C-5. Moreover, a methyl ester substitution at C-1 could be supported by HMBC correlations from H-2 (δ_H 6.74) and the methoxyl protons (δ_H 3.73) to the ester carbonyl carbon C-19 (δ_C 167.6). Two acetoxy groups were located at C-4 and C-10 due to the correlations of H-4 (δ_H 5.02) and H-10 (δ_H 4.74) to the corresponding ester carbonyl carbons (δ_C 170.5 and 170.7), respectively. Thus, a hydroxy group should be attached at C-9 to match the data of IR, NMR, and molecular formula. Therefore, the planar structure of **1** possessing a novel molecular skeleton was established. The relative configuration of compound **1** was determined from examination of NOESY correlations (Figure 3) and coupling constant-based configurational analysis. The geometry of the 1,2-double bond was assigned to be *E* from NOESY correlations of H-2 (δ_H 6.74) with one proton of H-3 (δ_H 2.26), the other proton of H-3 (δ_H 2.68) with one proton of H-12 (δ_H 2.21), but H-2 showed no interaction with H_2-12. The *Z* geometry of the 6,7-double bond was deduced on the basis of the coupling constant ($J = 11.2$ Hz), and the observed NOESY interaction between H-6 and H-7. Consideration of the biosynthetic pathway of **1** from related tortuosenes[23] (Scheme 1) made us assume the β-orientation of H_3-20 which showed NOESY correlations with both H-7 and

Table 1. ^{1}H NMR spectroscopic data of compound **1**–**6** ($CDCl_3$).

No	**1**[a]	**2**[a]	**3**[b]	**4**[b]	**5**[a]	**6**-A[a]	**6**-B
1							
2	6.74 dd (10.4, 6.0)	6.90 dd (9.6, 4.8)	3.04 d (8.0)	2.97 d (8.0)	2.90 dd (11.6, 8.0)	4.99 d (11.2)	5.80 d (9.2)
3α	2.26 m	2.51 m	6.65 d (8.0)	6.61 d (8.0)	6.95 d (11.6)	3.89 d (11.2)	3.09 d (9.2)
3β	2.68 m						
4	5.02 d (9.6)	4.92 dt (10.8, 2.4)					
5α	2.46 m	2.52 m	2.56 m	2.55 m	2.92 m	1.61 m	2.01 m
5β			2.90 td (13.0, 5.0)	2.88 td (12.5, 7.0)	2.30 t (13.2)	2.03 m	1.74 m
6	5.69 dd (11.2, 10.0)	5.10 t (11.6)	1.79 m (α) 1.93 m (β)	1.86 m	2.15 m (α) 1.13 m (β)	1.58 m (α) 1.74 m (β)	1.72 m (α) 1.23 m (β)
7	5.58 dt (11.2, 2.8)	5.94 dt (11.6, 3.6)	4.51 dd (11.5, 2.5)	4.53 dd (10.0, 4.5)	2.97 dd (11.2, 2.8)	5.02 dd (8.0, 4.0)	5.65 dd (12.0, 2.8)
8	2.52 m 2.08 m	2.33 m 2.12 m					
9α			1.18 m	1.71 m	1.08 m	1.94 m	2.08 m
9β			1.74 m	1.49 m	2.15 m		1.94 m
10α	4.74 d (9.6)	4.54 d (10.8)	1.92 m	1.95 m	1.62 m	2.34 m	2.76 m
10β			1.97 m	1.90 m		2.24 m	2.39 m
11	2.04 m 1.33 m	2.33 m 1.69 m	3.58 dd (11.0, 7.0)	3.68 brs	1.87 d (6.4)	6.20 dd (5.6, 5.2)	6.32 t (4.0)
12	2.43 m 2.21 m	2.62 m 2.18 m					
13	1.58 m	1.90 m 1.29 m	2.50 m 1.93 m	2.56 m 1.97 m	2.04 m 1.78 m	2.93 m 2.16 m	3.02 m 2.04 m
14α	2.38 m	2.34 m	1.91 m	1.88 m	1.74 m	2.58 m	1.90 m
14β		2.28 m	1.62 m	1.62 m	1.81 m	1.88 m	2.44 m
15			1.66 m	1.66 m	1.72 m	2.74 m	2.26 m
16	2.54 m	2.54 m	0.80 d (7.0)	0.80 d (7.0)	0.83 d (6.4)	1.03 d (7.2)	1.01 d (6.8)
17	1.06 d (6.8)	1.06 d (6.8)	0.96 d (6.5)	0.95 d (6.5)	0.78 d (6.4)	1.06 d (7.2)	1.04 d (6.8)
18	1.06 d (6.8)	1.06 d (6.8)					
19			1.28 s	1.28 s	1.00 s	1.39 s	1.35 s
20	1.27 s	1.18 s			1.25 s		
21	3.73 s	3.73 s			3.75 s		
4-OAc	2.11 s	2.15 s	3.78 s	3.78 s			
7-OAc			1.96 s	1.94 s		2.07 s	2.07 s
10-OAc	2.14 s	2.11 s					
11-OMe			3.27 s	3.29 s			
18-OMe						3.75 s	3.73 s

a) ^{1}H NMR spectrum was measured at 400 MHz. b) ^{1}H NMR spectrum was measured at 500 MHz.

H-10, suggesting the β-orientation of H-10 and upward orientation of H-6 and H-7. The coupling constant between H-5 and H-6 ($J = 10.0$ Hz) suggested an antiperiplanar orientation, while NOESY correlations between H-6 and H_2-13 (δ_H 1.58), implied the α-orientation of H-5. Furthermore, H-4 showed NOE correlations with H-2, H-5, H_2-13, and one proton of H-3 (δ_H 2.26) but not with H-6, while H-6 exhibited correlations with another proton of H-3 (δ_H 2.68), revealing H-4 and the proton of H-3 appearing at δ_H 2.26 were α-orientation. Additionally, a coupling constant of 9.6 Hz between H-4 and H-3β implied that they are *anti*-oriented, while the zero or very small J values between H-4 and H-5; H-4 and H-3α suggested *gauche* conformations of H-3α/H-4, and H-4/H-5 (Figure 3). Thus, the orientations of H-4, H-5, and H_2-13 were characterized as α-axial, α-axial, and β-equatorial, respectively. The absolute configuration of **1** was determined by comparison of the experimental and calculated electronic circular dichroism (ECD) spectra. Conformational searching using molecular mechanics with MMFF force field in the Spartan'14 program was carried out for compound **1**.[29] In a relative energy window of 0–3 Kcal/mol, the result showed 10 lowest energy conformers (Figure S45) meeting the requirements of the observed NOE correlations (Table S1). The lowest energy conformer (above 59.1% population) obtained was further refined by DFT optimization at the M06-2X/Def2-SVP level and the ECD spectrum was calculated by time-dependent DFT approach at the CAM-B3LYP/def2-TZVP level (including a PCM solvent model for MeOH).[30] The ECD spectrum calculated for the (4*S*,5*R*,9*R*,10*S*) absolute configuration of **1** was found to be opposite to the experimental curve (Figure 4), therefore, the absolute configuration of **1** was determined as (4*R*,5*S*,9*S*,10*R*).

Secotortuosene B (**2**), $[\alpha]_D^{25}$ +26.3 (*c* 0.43, $CHCl_3$), had the same molecular formula of $C_{25}H_{38}O_8$ (*m*/*z* 489.2462 $[M + Na]^+$), and similar IR absorptions at 3481, 1734, 1712,

Table 2. ^{13}C NMR spectra data of compounds **1**–**6** ($CDCl_3$).

	1[a)]	**2**[a)]	**3**[b)]	**4**[b)]	**5**[a)]	**6-A**[a)]	**6-B**
1	135.2 s	133.9 s	74.8 s	74.6 s	55.4 s	147.9 s	148.6 s
2	137.2 d	136.9 d	48.9 d	49.0 d	41.0 d	121.0 d	119.2 d
3	33.6 t	31.0 t	139.8 d	139.5 d	144.0 d	44.1 d	43.5 d
4	74.2 d	74.2 d	131.7 s	131.6 s	128.7 s	54.5 s	52.7 s
5	39.8 d	39.5 d	24.3 t	24.3 t	23.3 t	22.6 t	33.5 t
6	129.8 d	129.2 d	27.2 t	26.7 t	24.6 t	25.4 t	24.0 t
7	126.8 d	130.2 d	75.5 d	75.5 d	65.5 d	73.8 d	72.3 d
8	39.2 t	39.0 t	82.7 s	84.1 s	59.1 s	84.8 s	81.9 s
9	74.4 s	74.7 s	31.8 t	30.4 t	42.0 t	36.4 t	34.3 t
10	79.4 d	78.1 d	22.6 t	22.4 t	36.6 d	25.1 t	27.3 t
11	30.6 t	29.2 t	81.7 d	81.5 d	57.2 d	142.5 d	141.2 d
12	23.8 t	21.0 t	116.2 s	117.1 s	81.6 s	133.8 s	133.3 s
13	27.3 t	25.4 t	23.8 t	23.0 t	40.3 t	33.9 t	33.3 t
14	37.5 t	37.0 t	25.6 t	25.9 t	27.4 t	37.6 t	27.2 t
15	214.2 s	214.3 s	33.2 d	33.1 d	38.6 d	29.7 d	31.0 d
16	40.9 d	40.8 d	16.0 q	16.0 q	18.4 q	22.0 q	24.2 q
17	18.3 q	18.3 q	15.7 q	15.7 q	17.1 q	22.2 q	21.5 q
18	18.3 q	18.3 q	167.4 s	167.4 s	168.4 s	175.6 s	173.7 s
19	167.6 s	168.2 s	20.5 q	20.8 q	18.1 q	25.6 q	23.8 q
20	25.2 q	28.6 q	145.5 s	143.9 s	22.3 q	170.3 s	170.3 s
21	51.9 q	52.1 q	51.9 q	51.9 q	52.0 q		
4-OAc	21.1 q	21.1 q					
	170.5 s	170.5 s					
7-OAc			21.1 q	21.1 q		21.0 q	20.9 q
			169.8 s	169.4 s		167.1 s	167.0 s
10-OAc	21.0 q	21.0 q					
	170.7 s	170.7, C					
11-OMe			54.0 q	56.7 q			
18-OMe						52.2 q	51.0 q

a) ^{13}C NMR spectrum was measured at 100 MHz. b) ^{13}C NMR spectrum was measured at 125 MHz.

and 1240 cm^{-1} as those of compound **1**. The ^{1}H and ^{13}C NMR spectra (Table 1) of **2** showed signals similar to those of **1**, suggesting that both compounds could be stereoisomers. The key HMBC correlations from H-2, H_2-12, and methoxy protons to C-19; H-3 and H_2-13 to C-5; H_3-20 to C-8, C-9, and C-19; H_2-13, H_2-14, H_3-16, H_3-17, and H_3-18 to C-15, connecting the four COSY fragments as shown in Figure 2, confirmed the planar structure of **2**. The similar coupling constant between H-6 and H-7, and NOE correlations between H-12 and H-3; H-6 and H-7, but the absence of correlation between H-2 and H-12 (Figure 3), revealed the *trans* 1,2- and *cis* 6,7-double bonds in **2**, the same as those of **1**. The NOESY spectrum showed correlations between H-10 (δ_H 4.54) and H_3-20 (δ_H 1.18), implying the β-orientation of the methyl group at C-10. Without showing NOE correlation with H-7, H_3-20 showed an NOE interaction with a quasi-equatorial proton of H-8 (δ_H 2.12) as H_3-20 and H-8 are close in space. On the other hand, the other proton (δ_H 2.33) of H_2-8 showed an NOE correlation with H-5 (δ_H 2.52) which presented an antiperiplanar orientation with H-6 ($J = 11.6$ Hz), revealing the downward orientation of both olefinic protons H-7 and H-6, and the β-orientation of H-5 in **2**. Moreover, H-6 showed a stronger NOE correlation with H-4 (δ_H 4.92), suggesting the α-orientation of H-4, too. Thus, **2** was established as the 5-epimer of **1**. To explain why with the same configuration at C-9 of both compounds **1** and **2**, the NOE interaction displayed between H_3-20 and H-7 in compound **1** was absent in **2**, a model interchanging the positions of hydrogen atom and side chain substitution of **1** at C-5 only, was established as conformer **2′** (Figure 3). The conformer **2′** was shown to be unstable by the 1,3-diaxial steric repulsion between the 2- methyl-3-oxopentanyl substituent at C-5 with C-2 containing ring residue at C-3, and leading to the conversion of conformer **2′** to a more stable conformer **2**, in which the NOE interaction between H_3-20 and H-7 was not found due to the longer distance of H-7/H_3-20 in comparison with that of **1**. The above deduction was further supported by conformational searches for **2** using MMFF as the force field. In a relative energy window of 0–3 Kcal/mol, the results (Table S1) showed eleven lowest conformers for **2** (Figure S46), which can explain the observed NOE correlations. However, conformer **2′** was not shown in the above eleven lowest energy conformers, revealing that the side chain was fixed in a specific way due to a large barrier in **2′**, and making the conformer **2**, not **2′**, to be the adequate conformation for compound **2**. Furthermore, 6,7-double bonds of **1** and **2** were positioned at β and α face, respectively, which could be confirmed by the chemical shift of more downfield-shifted H-7 (δ_H 5.94) in **2** than in **1** (δ_H 5.58) due to the shorter distance between the hydroxyl group at C-10 and H-7. Similarly, the upfield-shifted H-6 (δ_H 5.10 in **2** and δ_H 5.69 in **1**) and the downfield-shifted H_2-13 of **2** (δ_H 1.90, 1.29 in **2** and δ_H 1.58 in **1**) was due to the spatial proximity of H-6 and 4-OAc in **1**, while H-6 was found

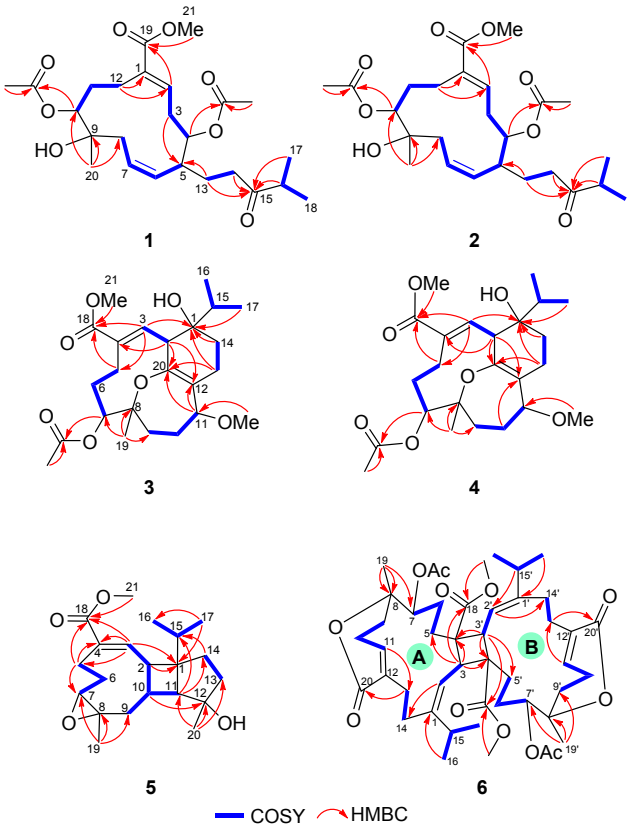

Figure 2. COSY and HMBC correlations of compounds **1**–**6**.

to be close to H_2-13 of the 2-methyl-3-oxopentanyl side chain in **2**, respectively. Therefore, secotortuosene B (**2**) was identified as a C-5 epimer of **1**.

Tortuosene C (**3**), $[\alpha]_D^{25}$ +104.3 (*c* 0.43, $CHCl_3$), presented a sodiated quasimolecular ion peak at *m*/*z* 459.2356 $[M + Na]^+$ in the HRESIMS experiment, consistent with the molecular formula of $C_{24}H_{36}O_7$, and seven degrees of unsaturation. Its IR spectrum exhibited absorptions at 3454 and 1715 cm^{-1}, revealing the presence of hydroxy and ester carbonyl functionalities, respectively. In ^{13}C NMR spectrum (Table 2), together with the DEPT and HSQC spectra, 24 carbon signals were assigned into four olefinic carbons (δ_C 116.2, 131.7, 139.8, and 145.5), four methyls (δ_C 15.7, 16.0, 20.5, and 21.1), six sp^3 methylenes (δ_C 22.6, 23.8, 24.3, 25.6, 27.2, and 31.8), four sp^3 methines (δ_C 33.2, 48.9, 75.5, and 81.7), two methoxyls (δ_C 51.9 and 54.0), and two oxygenated quaternary carbons (δ_C 74.8 and 82.7). Two carbonyl groups and two double bonds contribute four degrees of unsaturation, thus **3** should be a tricyclic compound. Detailed analysis of its NMR data including those from ^1H spectrum (Table 1) indicated that the structure of **3** is similar to that of tortuosene A,[23] except for the ketone group at C-11 position of tortuosene A was replaced by a methoxy group in **3**. The key proton sequence from H-9 through H-10 to H-11 was observed in the COSY spectrum (Figure 2). Furthermore, the molecular skeleton of **3** was established by analysis of its HMBC correlations (Figure 2), including the HMBC correlation from methoxy proton (δ_H 3.29) to C-11 (δ_C 81.5) which confirmed the C-11 position of the methoxy group. Thus, the planar structure of compound **3** was established as shown in Figure 2.

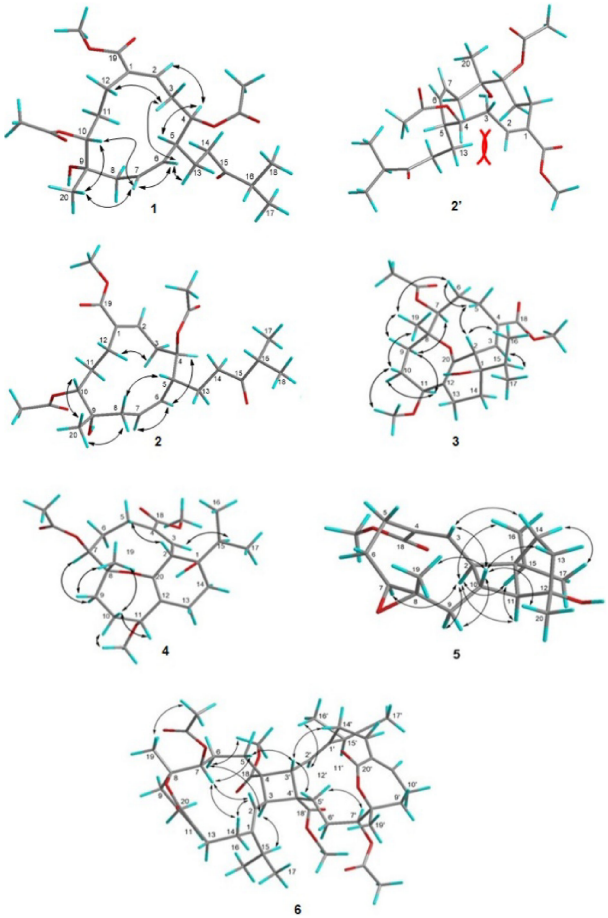

Figure 3. Main NOE correlations of compounds **1**–**6** and model of 5-*epi* of **1** (**2′**) with steric repulsion.

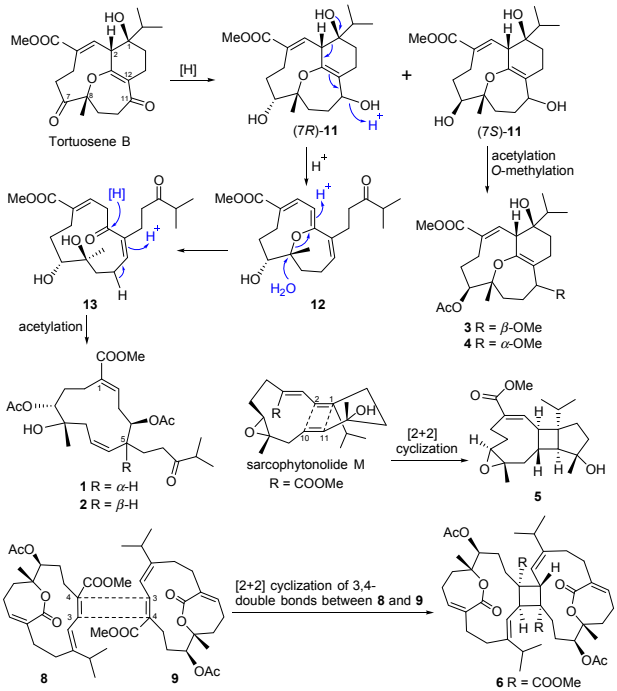

Scheme 1. Putative biosynthetic pathway for compounds **1**–**6**.

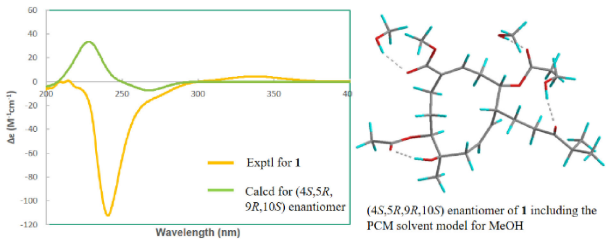

Figure 4. Experimental ECD spectrum of **1** compared with the spectrum calculated for (4*S*,5*R*,9*R*,10*S*)-**1** at B3LYP/Def2-TZVP including the PCM solvent model for MeOH.

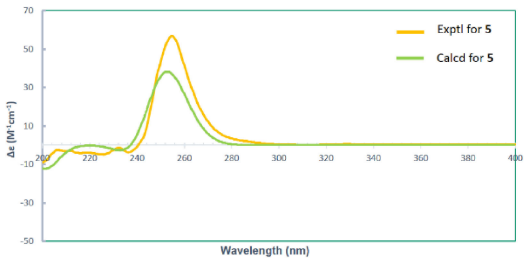

Figure 5. Experimental CD spectrum of **5** compared with the ECD spectrum calculated for the (1*S*,2*S*,7*S*,8*S*,10*R*,11*S*) enantiomer of **5**.

On the basis of the similarity of NMR data and biogenetic considerations, the stereochemistry of H_3-19 was assumed to be β-orientated as that of tortuosane derivatives.[23] The NOESY correlations of H_3-19/H-6β (δ_H 1.93), H-6β/H-5β (δ_H 2.90), and H-5β/H-2 (δ_H 3.04), suggested that the β-orientation of H-2 and *E* geometry of C-3/C-4 double bond. Also, H_3-19/H-9β (δ_H 1.74), while H-7 (δ 4.51) showed cross-peaks with H-6α (δ_H 1.79) and H-9α (δ_H 1.18) revealed the α-orientation of H-7. Furthermore, the identical NOE correlations of H-2/H-16, and H-3/H-15 in both **3** and tortuosene A, indicated the 1*R**,2*R** configuration of **3**. In addition, the NOE correlations of H_3-19/H-10β (δ_H 1.97), H-10β/11-OMe (δ 3.27), and H-9α/H-11 (δ_H 3.58) indicated that the methoxy group should be located on the β face at C-11. Based on the above findings and the shared biosynthetic pathway with tortuosane diterpenoids, the absolute configuration of compound **3** was determined as shown in Figure 1.

Tortuosene D (**4**) was isolated as a white solid with $[\alpha]_D^{25}$ +138.3 (*c* 0.43, $CHCl_3$). The molecular formula, $C_{24}H_{36}O_7$, was deduced from its HRESIMS (*m*/*z* 459.2356 $[M + Na]^+$, calcd 459.2359) data. The IR spectrum showed the presence of hydroxy (3491 cm^{-1}), ester carbonyl (1716 cm^{-1}), and olefinic (1643 cm^{-1}). The close ^1H and ^{13}C data of **4** and **3** (Tables 1 and 2) indicated they are isomers. The differences were the 11-OMe carbon signal downfield shifted to δ_C 56.7 in **4** (δ_C 54.0 in **3**), and the C-9 and C-20 signals upfield shifted to δ_C 30.4, 143.9 in **4** (δ_C 31.8, 145.5 in **3**), respectively. Additionally, in the ^1H NMR spectrum, the multiplicity and chemical shift of H-11 (δ_H 3.68, s) in **4** were different from that of **3** (δ_H 3.58, dd, $J = 11.0, 7.0$ Hz), which implied those two compounds are C-11 epimers. The above assumption was confirmed by NOE correlations (Figure 3) of H_3-19 (assumed as β-orientation)/H-9β (δ_H 1.49), H_3-19/H-10β (δ_H 1.90), H-10α (δ_H 1.95)/11-OMe (δ_H 3.29), and H-7 (δ_H 4.53)/H-9α (δ_H 1.71). Moreover, the minimal *J* values between H-11 and H-10α/H-10β agreed with their equal dihedral angles.[31] Therefore, the methoxy group at C-11 of **4** was assigned an α-orientation. Thus, the relative configuration of **4** was unambiguously established.

Tortuosumol (**5**), isolated as a colorless oil, has a molecular formula $C_{21}H_{32}O_4$ from its HRESIMS (*m*/*z* calcd 371.2198; found 371.2196, $[M + Na]^+$), implying six degrees of unsaturation. Its IR spectrum revealed the presence of hydroxy (ν_{max} 3451 cm^{-1}), carbonyl (ν_{max} 1701 cm^{-1}), and methyl (ν_{max} 1377 cm^{-1}) groups. The ^1H NMR, ^{13}C NMR and DEPT spectra (Tables 1 and 2) of **5** showed signals of five methyls (including one isopropyl and one methoxyl), five sp^3 methylenes, five sp^3 methines (including one oxymethine), one sp^2 methine, three sp^3 quaternary carbons, and two sp^2 quaternary carbons (including one ester carbonyl). A quaternary carbon signal at δ 168.4 indicated the presence of an ester carbonyl, while one trisubstituted double bond was also identified from carbon signals appearing at δ 128.7 (C) and 144.0 (CH). In the COSY spectrum, it was possible to identify four different structural units, which were assembled with the assistance of HMBC correlations (Figure 2). Key HMBC correlations from H-2 to C-1; H-3 to C-1, C-4, C-5, and C-18; H_2-5 to C-3, C-4, C-7, and C-18; H_3-19 to C-7, C-8, and C-9; H-10 to C-3 and C-12; H-11 to C-9, C-12, C-14, and C-15; H_2-14 to C-1 and C-15 as well as both H_3-16 and H_3-17 to C-1 and C-15 permitted the establishment of a tetradecahydrocyclopenta[3′,4′]cyclobuta[1′,2′:4,5]-cyclonona[1,2-*b*]-oxirene carbon skeleton (Figure 2).[32] Furthermore, the methoxy group positioned at C-18 was confirmed from the HMBC correlation of methoxy protons (δ_H 3.75, s) to the carbonyl carbon at δ_C 168.4. Moreover, an epoxide at C-7 and C-8, as well as a hydroxy group at C-20 were deduced from their chemical shifts and mass data. Thus, the planar structure of **5** was established as a tricarbocyclic diterpene. The relative configuration of **5** was elucidated by the analysis of NOE correlations, as shown in Figure 3. Assuming the *a*-orientation of H-2 (δ 2.90), which showed NOE interactions with H-7 (δ 2.97), H-9*a* (δ 1.08), H-11 (δ 1.87), H-15 (δ 1.72), and H_3-16 (δ 0.83). Thus, H-7, H-11, and H-15 should be positioned on the α face. On the other hand, the coupling constant of $J_{H\text{-}2/H\text{-}10}$ (8.0 Hz) revealing the *trans* configuration of H-2 and H-10, and implied H-10 was placed on the β-side of the structure. In addition, H-10 showed NOESY correlations with H-9β (δ 2.15), H-13 (δ 2.04), H_3-19 (δ 1.00), and H_3-20 (δ 1.25), as well as H-3 positioned as a quasi-axial β orientation, also showed correlations with H-10 and H-14α (δ1.74, m) revealed H_3-19 and H_3-20 were on the β face. This result was confirmed by the chemical shift of H-10 (δ 1.62) in **5** that was upfield-shifted from that of sarcotroate A [H-10 (δ 2.19)], and the absence of NOE correlation between H_3-17 and H_3-20 in **5**.[32] Based on the above findings, the relative configuration of **5** was determined. The CD spectrum of **5** in methanol displays a positive Cotton effect at 255 ($\Delta\varepsilon = 56.8$). The calculated ECD spectrum of **5** was found to match well with the experimental ECD (Figure 5), allowing the absolute configuration of **5** to be assigned as (1*S*,2*S*,7*S*,8*S*,10*R*,11*S*).

Bistortuolide cyclobutane A (**6**) was afforded as a white amorphous powder. The molecular formula $C_{46}H_{64}O_{12}$ of **6** was determined by HRESIMS (*m*/*z* calcd 831.4295; found

831.4288, $[M + Na]^+$), adequate for 15 degrees of unsaturation. The IR spectrum of **6** showed the presence of two carbonyl groups (ν_{max} 1726 and 1690 cm^{-1}). The ^{13}C NMR spectroscopic data of **6** (Table 2) revealed the presence of 46 carbons, including 10 methyls, 12 methylenes, 10 methines, and 14 quaternary carbons. Its NMR spectra showed the signals of two acetoxyls (δ_H 2.07, 2.07; δc 167.0, 167.1 C; 20.9, 21.0, CH_3), two carbomethoxy groups (δ_H 4.99, d, $J = 11.2$ Hz; 5.80, d, $J = 9.2$ Hz; 6.20, dd, $J = 5.6$, 5.2 Hz; 6.32, t, $J = 4.0$ Hz; δc 147.9, C, 121.0, CH; 142.5, CH, 133.8, C; 148.6, C, 119.2, CH; 141.2, CH, 133.3, C), and four additional carbonyl carbons (δc 170.3, 170.3, 173.7, and 175.6). All of the above findings and ^1H NMR data (Table 1) suggested that **6** might be a pentacyclic compound with a biscembranoid skeleton. The COSY signals reveal the presence of ten structural units from H-2 to H-3; H_2-5 via H_2-6 and H-7; H_2-9 via H_2-10 and H-11; H_2-13 to H_2-14; isopropyl protons H_3-16 and H_3-17 via H-15; H-2′ to H-3′; H_2-5′ via H_2-6′ and H-7′; H_2-9′ via H_2-10′ and H-11′; H_2-13′ to H_2-14′, and other isopropyl protons H_3-16′ and H_3-17′ via H-15′. These units could be assembled by HMBC correlations of H-2/C-14; H-3/C-4, C-5, C-18, and C-4′; H-11/C-13; H_2-13/C-20; H-15/C-2; H_3-16 and H_3-17/C-1; H_3-19/C-7, C-8 and C-9; 18-OMe/C-18; H-2′/C-14′; H-3/C-4, C-4′, C-5′, and C-18′; H-11′/C-13′; H_2-13′/C-20′; H-15′/C-2′; H_3-16′ and H_3-17′/C-1′; H_3-19′/C-7′, C-8′, and C-9′; 18′-OMe/C-18′. Thus, **6** was suggested to possess two 14-membered cembranoidal units with each one containing an α, β-unsaturated-ε-lactone ring. Moreover, key HMBC correlations from both H-3 and H-3′ to C-4, C-5, C-18, C-4′, and C-5′, and C-5, C-4, C-4′, and C-18′, respectively, leading to the construction of the four-membered ring (C-3/C-4/C-3′/C-4′). Therefore, the gross structure of **6** possessing a novel cyclobutanyl biscembranoid skeleton was established (Figure 2). The configuration of **6** was further determined by analysis of NOE correlations and by referring to the previous studies from a literature survey.[28] From the *R* configuration of C-8, the β-orientated H_3-19 (δ_H 1.39) showed an NOE interaction with 7-OAc (δ_H 2.07), but not with H-7 (δ_H 5.02), revealing that the acetoxy group should be β-orientated and H-7 should be equatorially orientated inside the ring. The NOE correlations of H-7/H-2 (δ_H 4.99), H-7/H-14a (δ_H 1.88), and H-7/H-5a (δ_H 2.03), implied the upward orientation of H-2 and β-orientated positions of H-5a and H-14a. Furthermore, H-3 exhibited NOE correlations with H-15 (δ_H 2.74), but neither correlated with H-2 nor H-3′ (δ_H 3.09), while H-5a showed NOE correlation with H-3′, revealing the α-orientation of H-3, β-orientation of H-3′ and the downward orientation of the isopropyl unit attached at C-1. Additionally, the NOE correlations of H-3/H-6a (δ_H 1.58), H-6a/18-OMe (δ_H 3.75), reflected the α-orientation of H-6a and 4-COOMe. The *Z* geometry of the 1,2-double bond was deduced from H-2 which showed NOE correlation with one proton of H-14 (δ_H 1.88). Moreover, the NOE correlations of H-3′ with H-5a′ (δ_H 1.74) and H-14′ (δ_H 2.44), implied these protons should be β-orientated. Also, the H-7′ (δ_H 5.65) showed a weak NOE correlation with α-orientated H-5b′ (δ_H 2.01), but not correlated with H_3-19′ (δ_H 1.35), revealing the β-orientation of both 7′-OAc and H_3-19′. The NOE correlations between H-11 and H-13, and H-11′ and H-13′, confirmed the *cis* geometry for both 11,12 and 11′,12′-double bonds. Additionally, the *E* geometry of the 1′,2′-double bond was assigned since the NOE interaction between H-2′ and H_3-16′ was observed. According to the above-described evidence and by comparison of the NMR spectral data of cemberanoides containing the same ε-lactone ring,[33,34] the chemical structure of **6** was unambiguously established. A plausible biosynthetic pathway for **1**–**6** was proposed and illustrated in Scheme 1. The C-7 and C-11 ketone of tortuosene B could be reduced to form triol **11**. The intermediate (7*S*)-**11** further underwent *O*-methylation and acetylation to yield C-11 epimers **3** and **4**. On the other hand, acid-catalyzed dehydration of (7*R*)-**11** would form a cation at C-11 and induce the migration of (12,20)-double to C-11 and C-12, and the subsequent cleavage of the 1,2-single bond to form a 12-membered trienyl ketone **12**. The protonation of **12** at the β carbon of enol ether double bond can further trigger the hydrolysis of ether ring and the following addition of H_2O to form **13** and lead to the formation of **1** and **2** as illustrated in Scheme 1. Besides, **5** might be transformed from sarcophytonolide M via an intramolecular [2+2] cyclization,[32] while **6** might originate via an intermolecular [2+2] cyclization between sartrolide G (**8**) and emblide (**9**) as depicted in the proposed hypothetical pathway in Scheme 1.[34,35]

In vitro cytotoxic activity of isolated diterpenoids was evaluated against four human cancer cell lines, including human erythroleukemia (K562), leukemia (CCRF-CEM), breast carcinoma (T47D), and lymphoid T (MOLT 4) carcinoma cells, using the Alamar Blue assay. However, the results reveal that compound **5** showed inhibition toward MOLT 4 cancer cell lines ($IC_{50} = 21.7$ μM), and **6** showed inhibitions toward murine leukemia (P388), human myelogenous leukemia (K562), and human colon carcinoma (HT-29) cancer cell lines with IC_{50} values of 8.5, 9.2, and 34.1 μM, respectively. The in vitro anti-inflammatory effects of isolates were evaluated by suppressing *N*-Formyl-Met-Leu-Phe/cytochalasin B (fMLF/CB)-induced superoxide radical anion ($O_2^{\bullet-}$) generation and elastase release in human neutrophils. At a concentration of 10 μM, compounds **3**, **5**–**7** showed inhibitions (18.22 ± 2.62, 16.69 ± 5.88, 64.72 ± 5.44, and 18.90 ± 2.92%, respectively) toward superoxide anion generation. At the same concentration, compounds **3**, **6**, and **7** also displayed inhibitions (22.46 ± 3.21, 66.45 ± 3.63, and 29.22 ± 6.12%, respectively) against fMLF-induced elastase release. Additionally, the IC_{50} values of **6** against the generation of superoxide anion and elastase release were 5.94 ± 1.36 and 6.17 ± 0.48 μM, respectively. Moreover, compounds **1**–**10** were further assayed for the anti-inflammatory activity by evaluating the NO (nitric oxide) production in LPS-induced RAW 264.7 cells. As a result, these isolates were found to be not cytotoxic on RAW 264.7 macrophages at the dose of 100 μM, while compounds **6**, **7**, and **10** were found to inhibit NO release with IC_{50} values of 36.7, 37.0, and 47.5 μM, respectively. All of the results reveal that *S. tortuosum* could produce a variety of bioactive metabolites whereas compound **6** is worthy of further research and development as a promising drug candidate in the future.

3. Conclusion

In summary, six new diterpenoids including two novel 12-membered skeleton compounds secotortuosenes A and B (**1** and **2**), two new tortuosane diterpenoids, tortuosenes C and D (**3** and **4**), tortuosumol (**5**), and one novel cyclobutane

biscembranoid (**6**), together with four known compounds named ketoemblide (**7**), sartrolide G (**8**), emblide (**9**), and sarcrassin E (**10**) were isolated from the ethyl acetate extract of soft coral *S. tortuosum*. Moreover, compounds **1** and **2** represent an unprecedented skeleton of a 12-membered ring connecting a 2-methyl-3-oxopentanyl group, which was assumed to be formed from tortuosane diterpenoids. The absolute configuration of **1** and **5** were determined by TDDFT ECD calculations. Compound **6**, possessing a novel cyclobutane biscembranoid skeleton, was assumed to be biosynthesized from two precursors **8** and **9**. Among them, compounds **5** and **6** exhibited inhibitory activity towards a limited panel of cancer cell lines. Compounds **3**, **5**–**7**, and **10** were shown to exhibit anti-inflammatory activities while **6** was shown to be the most active one. The discovery of the unprecedented molecular skeleton of **6** from [2+2] cyclization of two corresponding 1,3-butadienyl cembranoids might shed light on the discovery of more structurally similar natural biscembranoids via similar biosynthetic pathway from other 1,3-butadienyl cembranoids. With the high biological and chemical diversity from the present study and previous ones for the corals of the genus *Sarcophyton*,[19,36–39] it is important to more extensively explore the new secondary metabolites and unveil the bioactivities for compounds from this genus, for the future development of new medicines from marine organisms.

4. Experimental

General Experimental Procedures. Optical rotations and IR spectra were recorded on a Jasco P-1020 polarimeter and an FT/IR-4100 infrared spectrophotometer (Jasco Corporation, Tokyo, Japan), respectively. 1D and 2D NMR were acquired with a Varian Unity INOVA 500 FT-NMR (Varian Inc., Palo Alto, CA, USA) at 500 and 125 MHz for ^{1}H and ^{13}C, respectively; or a Varian 400 MR FT-NMR instrument at 400 MHz and 100 MHz for ^{1}H and ^{13}C, respectively. The data of low-resolution electron spray ionization mass spectroscopy (LRESIMS) were measured with a Bruker APEX II mass spectrometer, while high-resolution mass spectra were obtained with a Bruker Apex-Qe 9.4 T mass spectrometer. Silica gel 60 (200–300 mesh, Darmstadt, Merck) and RP-C_{18} (200–300 mesh, Darmstadt, Merck) were used for open-column chromatography (CC). Fractions were monitored by TLC using precoated silica gel plates (Kieselgel 60 F_{254}, 0.2 mm, Merck, Darmstadt, Germany). High-performance liquid chromatography was performed on a Hitachi L-2455 HPLC apparatus with a Supelco C_{18} column (ODS-3, 5 µm, 250 × 20 mm; Sciences Inc., Tokyo, Japan).

Animal Material. The soft coral *Sarcophyton tortuosum* (1.3 kg, wet weight) was collected by scuba diving at a depth of 10–15 m along the coast of Lanyu Island of Taiwan in August 2008, and authenticated by Prof. Dr. Chang-Feng Dai (Institute of Oceanography, National Taiwan University, Taipei, Taiwan). The samples were stored in a freezer until extraction.

Extraction and Isolation. The frozen organisms of *S. tortuosum* were minced and extracted repeatedly (1L) with ethyl acetate (EtOAc) to obtain a crude product (10.2 g), which was fractionated to yield 25 fractions (F1–F25) according to the previously reported procedure.[23] By examination of ^{1}H NMR spectra together with TLC analysis on all obtained fractions, fractions F16–F20 (yielded from hexanes-EtOAc = 4:1, 3:1, 2:1, 1:1, and 1:2, respectively) were selected for further isolation. Fractions F18 and F19 were combined and separated by chromatography on Si gel using *n*-hexane-EtOAc (3:1) and then *n*-hexane-acetone (6:1 and 3:1) as eluents yielded three subfractions F18A, F18B, and F18C. Subfraction F18A was purified by normal-phase HPLC (*n*-hexane-EtOAc, 5:2) to give compound **1** (2.8 mg), F18B was purified by normal-phase HPLC (*n*-hexane-EtOAc, 3:1) to give compound **6** (2.5 mg), while subfraction F18C was purified by normal-phase HPLC (*n*-hexane-acetone, 3:1) to afford **2** (1.5 mg). The fraction F20, eluting from hexanes-EtOAc = 1:2, was subjected to purification with a C_{18} open column eluting with H_2O and MeOH (1:1) followed by normal phase HPLC (*n*-hexane-EtOAc, 3:1) to afford **3** (1.5 mg) and **4** (1.5 mg). Fraction F16 was purified using Si gel open column (hexanes-EtOAc, 5:1) to yield a subfraction which was further separated by semipreparative NP-HPLC eluting with *n*-hexane-EtOAc (5:1) to afford a fraction (F16AA). This subfraction was purified by normal phase HPLC (*n*-hexane-EtOAc, 3:1) to give compound **7** (5.2 mg). The further purification of fraction F17 was carried out on a silica gel open column with elution of *n*-hexane-EtOAc (3:1) to give two subfractions F17A and F17B. Compounds **8** (2.9 mg) and **9** (30.1 mg) were obtained from chromatography of subfraction F17A using semi-preparative HPLC (*n*-hexane-EtOAc, 5:1), while F17B was conducted on semi-preparative HPLC (*n*-hexane-acetone, 5:1) to obtain compounds **5** (4.5 mg) and **10** (20.0 mg).

Secotortuosene A (1): White solid; mp 69–71 °C; UV λ_{max} (MeOH) (log ε) 221 (3.60) nm; $[\alpha]_D^{25}$ +22.2 (*c* 0.8, $CHCl_3$); IR (KBr) ν_{max} 3496, 2969, 1736, 1712, 1239 cm^{-1}; ^{1}H and ^{13}C NMR spectroscopic data ($CDCl_3$) are shown in Tables 1 and 2; HREIMS *m*/*z* 489.2462 $[M + Na]^+$ (calcd for $C_{25}H_{38}O_8Na$, 489.2464).

Secotortuosene B (2): White solid; mp 69–71 °C; UV λ_{max} (MeOH) (log ε) 220 (4.10) nm; $[\alpha]_D^{25}$ +26.3 (*c* 0.43, $CHCl_3$); IR (KBr) ν_{max} 3482, 2962, 1735, 1712, 1241, 1206 cm^{-1}; ^{1}H and ^{13}C NMR spectroscopic data ($CDCl_3$) are shown in Tables 1 and 2; HREIMS *m*/*z* 489.2462 $[M + Na]^+$ (calcd for $C_{25}H_{38}O_8Na$, 489.2464).

Tortuosene C (3): White solid; mp 64–66 °C; UV λ_{max} (MeOH) (log ε) 257 (3.80), 218 (4.10); $[\alpha]_D^{25}$ +104.3 (*c* 0.43, $CHCl_3$); IR (KBr) ν_{max} 3454, 2931, 1715, 1250 cm^{-1}; ^{1}H and ^{13}C NMR spectroscopic data ($CDCl_3$) are shown in Tables 1 and 2; HREIMS *m*/*z* 459.2356 $[M + Na]^+$ (calcd for $C_{24}H_{36}O_7Na$, 459.2359).

Tortuosene D (4): White solid; mp 64–66 °C; UV λ_{max} (MeOH) (log ε) 257 (3.80), 218 (4.10) nm; $[\alpha]_D^{25}$ +138.3 (*c* 0.43, $CHCl_3$); IR (KBr) ν_{max} 3491, 2931, 1716 cm^{-1}; ^{1}H and ^{13}C NMR spectroscopic data ($CDCl_3$) are shown in Tables 1 and 2; HREIMS *m*/*z* 459.2356 $[M + Na]^+$ (calcd for $C_{24}H_{36}O_7Na$, 459.2359).

Tortuosumol (5): Colorless oil; UV λ_{max} (MeOH) (log ε) 231 (4.30) nm; $[\alpha]_D^{25}$ +124.0 (*c* 0.90, $CHCl_3$); IR (KBr) ν_{max} 3449, 2956, 1702 cm^{-1}; ^{1}H and ^{13}C NMR spectroscopic data ($CDCl_3$) are shown in Tables 1 and 2; HREIMS *m*/*z* 371.2196 $[M + Na]^+$ (calcd for $C_{21}H_{32}O_4Na$, 371.2198).

Bisotrtuolide cyclobutane A (6): White solid; UV λ_{max} (MeOH) (log ε) 286 (3.20), 206 (4.30) nm; $[\alpha]_D^{25}$ +55.8

(c 0.71, $CHCl_3$); IR (KBr) ν_{max} 2957, 1726, 1690 cm^{-1}; ^1H and ^{13}C NMR spectroscopic data ($CDCl_3$) are shown in Tables 1 and 2; HREIMS m/z 831.4288 $[M + Na]^+$ (calcd for $C_{46}H_{64}O_{12}Na$, 831.4295).

DFT and TD-DFT Calculations. Geometry optimizations were carried out at the M06-2X/Def2-SVP level of theory. Vibrational frequency calculations at the same level of theory were performed to confirm that the obtained structures are local minima on the potential energy surfaces. The ECD spectra were simulated by using the time-dependent DFT (TD-DFT) approach at the CAM-B3LYP/Def2-TZVP level of theory. The range-separated functional CAM-B3LYP has been recommended for ECD calculations.[30] While the bare structure of compound **5** was adopted as a model, additional three and four explicit methanol solvent molecules were added to compounds **1** and **2**, respectively, to reproduce the experimental ECD spectra. The bulk solvent effect of methanol was taken into account with the integral equation formalism variant polarizable continuum model (IEF-PCM). All calculations were done by the Gaussian 09 program.[40]

Cytotoxic Assay. Cytotoxicity assays were performed according to the published Alamar Blue assay protocol.[41,42] Cell lines including murine leukemia (P388), human chronic myelogenous (K562), human colon carcinoma (HT-29), human lung adenocarcinoma (A549), and lymphoblastic leukemia (MOLT-4) were purchased from the American Type Culture Collection. Cancer cells were seeded into a 96-well microtiter plate with flat bottoms (Thermo Scientific Nunc MicroWell plate) at densities of 5×10^3 to 1×10^4 cells per well and were incubated in a humidified, 5% CO_2 atmosphere incubator at 37 °C for 15 h. After that, cancer cells of each well were treated with test compounds dissolved in DMSO. After 3 days of culture, attached cells were incubated with Alamar Blue (10 μL/well,) for 4 h. The absorbance at 595 nm was measured using a microplate reader.

Superoxide Anion Generation in Activated Human Neutrophils. Neutrophils (6×10^5 cells/mL) incubating with 0.6 mg/mL ferricytochrome c and 1 mM Ca^{2+} in HBSS at 37 °C were treated with the isolates for 5 min and were primed by 1 μg/mL cytochalasin B (CB) for 3 min before being activated by 100 nM fMLF for 10 min. The amount of superoxide anion generation was measured by the absorbance at 550 nm (U-3010, Hitachi, Tokyo, Japan).[43,44]

Elastase Release in Activated Human Neutrophils. Neutrophils (6×10^5 cells/mL) incubated (with 100 μM MeO-Suc-Ala-Ala-Pro-Val-*p*-nitroanilide and 1 mM Ca^{2+}) in HBSS at 37 °C were treated with the tested compound for 5 min. Neutrophils were then activated with fMLF (100 nM)/CB (0.5 μg/mL) for 10 min. The amount of elastase release was measured by the absorbance at 405 nm (U-3010, Hitachi, Tokyo, Japan).[44]

Anti-NO Production of the Inflammatory Activity. A density of 2×10^5 cells/well of RAW 246.7 cells were plated into 96-well plates and incubated for 2 hours. The cells were treated with samples for 1 hour and then incubated for 1 day in fresh DMEM with or without 1 μg/mL of LPS. According to the Griess reaction, the NO production was measured by nitrite concentration of the culture medium.[45] Briefly, cell culture supernatant was reacted with Griess reagent [1:1 mixture of 0.1% *N*-(1-naphthyl)ethylene-diamine dihydrochloride in water and 1% sulfanilamide in 5% phosphoric acid] in a ratio of 1:1 in 96-well plate, and absorbance was examined by an ELISA reader under 540 nm.[46]

We thank Prof. Fang-Rong Chang of Kaohsiung Medical University for technical assistance with the Spartan'14 program. Financial support for this work was provided by National Science Council (NSC 100-2320-B-110-001-MY2), the Ministry of Science and Technology (MOST 108-2320-B110-003-MY2), and the Ministry of Education (97C03031 3) of Taiwan award to J.-H. Sheu.

Supporting Information

Copies of HRESIMS and 1D and 2D NMR spectra of **1**–**6**. Details for the MMFF conformational searching for **1** and **2**. This material is available on https://doi.org/10.1246/bcsj.20210261.

References

# These authors contributed equally to this work.

1 B. Tursch, A. Tursch, *Mar. Biol.* **1982**, *68*, 321.

2 C. S. McFadden, J. A. Sánchez, S. C. France, *Integr. Comp. Biol.* **2010**, *50*, 389.

3 J. C. Coll, *Chem. Rev.* **1992**, *92*, 613.

4 P. W. Sammarco, J. C. Coll, *J. Chem. Ecol.* **1990**, *16*, 273.

5 Z. D. Dinesen, *Coral Reefs* **1983**, *1*, 229.

6 A. Migné, D. Davoult, *Oceanol. Acta* **1997**, *20*, 453.

7 J. D. Ros, J. Romero, E. Ballesteros, J. M. Gili, *Diving in blue water: the benthos*, R. Margalef (Ed.), The Western Mediterranean, Pergamon Press, Oxford, **1985**, pp. 233–295.

8 Y. Benayahu, Y. Loya, *Bull. Mar. Sci.* **1981**, *31*, 514.

9 S. Aratake, T. Tomura, S. Saitoh, R. Yokokura, Y. Kawanishi, R. Shinjo, J. D. Reimer, J. Tanaka, H. Maekawa, *PLoS One* **2012**, 7e30410.

10 M. Slattery, J. B. McClintock, *Mar. Biol.* **1995**, *122*, 461.

11 B. Fleury, J. Coll, P. Sammarco, *Mar. Ecol. (Berl.)* **2006**, *27*, 204.

12 C. C. Peng, C. Y. Huang, A. F. Ahmed, T. L. Hwang, C. F. Dai, J. H. Sheu, *Mar. Drugs* **2018**, *16*, 276.

13 F. Ye, J. Li, Y. Wu, Z. D. Zhu, E. Mollo, M. Gavagnin, Y. C. Gu, W. L. Zhu, X. W. Li, Y. W. Guo, *Org. Lett.* **2018**, *20*, 2637.

14 I. G. Rodrigues, M. G. Miguel, W. Mnif, *Molecules* **2019**, *24*, 781.

15 L. F. Liang, Y. W. Guo, *Chem. Biodiversity* **2013**, *10*, 2161.

16 M. Shaaban, F. Y. Yassin, M. M. Soltan, *Nat. Prod. Res.* **2020**, *34*, 1.

17 T. Y. Huang, C. Y. Huang, C. H. Chao, C. C. Lin, C. F. Dai, J. H. Su, P. J. Sung, S. H. Wu, J. H. Sheu, *Mar. Drugs* **2020**, *18*, 452.

18 W. Li, Y. H. Zou, M. X. Ge, L. L. Lou, Y. S. Xu, A. Ahmed, Y. Y. Chen, J. S. Zhang, G. H. Tang, S. Yin, *Mar. Drugs* **2017**, *15*, 85.

19 Y. A. Elkhawas, A. M. Elissawy, M. S. Elnaggar, N. M. Mostafa, E. Al-Sayed, M. M. Bishr, A. N. B. Singab, O. M. Salama, *Mar. Drugs* **2020**, *18*, 41.

20 X. Liu, J. Zhang, Q. Liu, G. Tang, H. Wang, C. Fan, S. Yin, *Molecules* **2015**, *20*, 13324.

21 S. S. Sawant, P. W. Sylvester, M. A. Avery, P. Desai,

D. T. A. Youssef, K. A. El Sayed, *J. Nat. Prod.* **2004**, *67*, 2017.
22 K. H. Lai, W. J. You, C. C. Lin, M. El-Shazly, Z. J. Liao, J. H. Su, *Mar. Drugs* **2017**, *15*, 327.
23 K. H. Lin, Y. J. Tseng, B. W. Chen, T. L. Hwang, H. Y. Chen, C. F. Dai, J. H. Sheu, *Org. Lett.* **2014**, *16*, 1314.
24 Z. Xi, W. Bie, W. Chen, D. Liu, L. van Ofwegen, P. Proksch, W. Lin, *Mar. Drugs* **2013**, *11*, 3186.
25 Y. Uchio, M. Nitta, M. Nakayama, T. Iwagawa, T. Hase, *Chem. Lett.* **1983**, 613.
26 L. F. Liang, L. F. Lan, O. Taglialatela-Scafati, Y. W. Guo, *Tetrahedron* **2013**, *69*, 7381.
27 J. A. Toth, B. J. Burreson, P. J. Scheuer, J. Finer-Moore, J. Clardy, *Tetrahedron* **1980**, *36*, 1307.
28 C. Zhang, J. L. Su, Y. Liang, X. Yang, K. Zheng, L. Zeng, *J. Nat. Prod.* **2006**, *69*, 1476.
29 T. A. Halgren, R. B. Nachbar, *J. Comput. Chem.* **1996**, *17*, 587.
30 G. Pescitelli, T. Bruhn, *Chirality* **2016**, *28*, 466.
31 R. M. Silverstein, G. C. Bassler, *J. Chem. Educ.* **1962**, *39*, 546.
32 L. F. Liang, T. Kurtán, A. Mándi, L. G. Yao, J. Li, W. Zhang, Y. W. Guo, *Org. Lett.* **2013**, *15*, 274.
33 L. F. Liang, T. Kurtán, A. Mándi, L. G. Tao, J. Li, L. F. Lan, Y. W. Guo, *Tetrahedron* **2018**, *74*, 1933.
34 L. F. Liang, L. F. Lan, O. Taglialatela-Scafati, Y. W. Guo, *Tetrahedron* **2013**, *69*, 7381.
35 L. L. Sun, W. S. Li, J. Li, H. Y. Zhang, L. G. Yao, H. Luo, Y. W. Guo, X. W. Li, *J. Org. Chem.* **2021**, *86*, 3367.
36 C. C. Peng, C. Y. Huang, A. F. Ahmed, T. L. Hwang, J. H. Sheu, *Mar. Drugs* **2020**, *18*, 573.
37 T. Y. Huang, C. Y. Huang, S. R. Chen, J. R. Weng, T. H. Tu, Y. B. Cheng, S. H. Wu, J. H. Sheu, *Mar. Drugs* **2021**, *19*, 8.
38 G. D. Sala, F. Agriesti, C. Mazzoccoli, T. Tataranni, V. Costantino, C. Piccoli, *Mar. Drugs* **2018**, *16*, 467.
39 K. N. Maloney, R. T. Botts, T. S. Davis, B. K. Okada, E. M. Maloney, C. A. Leber, O. Alvarado, C. Brayton, A. M. Caraballo-Rodríguez, J. V. Chari, B. Chicoine, J. C. Crompton, S. R. Davis, S. M. Gromek, V. Kurnianda, K. Quach, R. M. Samples, V. Shieh, C. M. Sultana, J. Tanaka, P. C. Dorrestein, M. J. Balunas, C. S. McFadden, *J. Nat. Prod.* **2020**, *83*, 693.
40 M. J. Frisch, G. W. Trucks, H. B. Schlegel, G. E. Scuseria, M. A. Robb, J. R. Cheeseman, G. Scalmani, V. Barone, G. A. Petersson, H. Nakatsuji, X. Li, M. Caricato, A. Marenich, J. Bloino, B. G. Janesko, R. Gomperts, B. Mennucci, H. P. Hratchian, J. V. Ortiz, A. F. Izmaylov, J. L. Sonnenberg, D. Williams-Young, F. Ding, F. Lipparini, F. Egidi, J. Goings, B. Peng, A. Petrone, T. Henderson, D. Ranasinghe, V. G. Zakrzewski, J. Gao, N. Rega, G. Zheng, W. Liang, M. Hada, M. Ehara, K. Toyota, R. Fukuda, J. Hasegawa, M. Ishida, T. Nakajima, Y. Honda, O. Kitao, H. Nakai, T. Vreven, K. Throssell, J. A. Montgomery, Jr., J. E. Peralta, F. Ogliaro, M. Bearpark, J. J. Heyd, E. Brothers, K. N. Kudin, V. N. Staroverov, T. Keith, R. Kobayashi, J. Normand, K. Raghavachari, A. Rendell, J. C. Burant, S. S. Iyengar, J. Tomasi, M. Cossi, J. M. Millam, M. Klene, C. Adamo, R. Cammi, J. W. Ochterski, R. L. Martin, K. Morokuma, O. Farkas, J. B. Foresman, D. J. Fox, *Gaussian 09, Revision D.01*, Gaussian, Inc., Wallingford CT, **2013**.
41 G. R. Nakayama, M. C. Caton, M. P. Nova, Z. Parandoosh, *J. Immunol. Methods* **1997**, *204*, 205.
42 J. O'Brien, I. Wilson, T. Orton, F. Pognan, *Eur. J. Biochem.* **2000**, *267*, 5421.
43 H. P. Yu, P. W. Hsieh, Y. J. Chang, P. J. Chung, L. M. Kuo, T. L. Hwang, *Free Radical Biol. Med.* **2011**, *50*, 1737.
44 S. C. Yang, P. J. Chung, C. M. Ho, C. Y. Kuo, M. F. Hung, Y. T. Huang, W. Y. Chang, Y. W. Chang, K. H. Chan, T. L. Hwang, *J. Immunol.* **2013**, *190*, 6511.
45 H. K. Kim, B. S. Cheon, Y. H. Kim, S. Y. Kim, H. P. Kim, *Biochem. Pharmacol.* **1999**, *58*, 759.
46 Y. H. Hsieh, P. M. Kuo, S. C. Chien, L. F. Shyur, S. Y. Wang, *Phytomedicine* **2007**, *14*, 675.

